Synthesis, Characterization, and Hydrodesulfurization Activity of New Mesoporous Carbon Supported Transition Metal Sulfide Catalysts

Murid Hussain[†,‡] **and Son-Ki Ihm***[,†]

National Research Laboratory for Environmental Catalysis, Department of Chemical and Biomolecular Engineering, Korea Advanced Institute of Science and Technology (KAIST), 373-1 Gusung-dong, Yusung-gu, Daejeon 305-701, South Korea

The potential of sulfided Mo, Co, and CoMo catalysts supported on two different carbon mesostructures by KAIST-1 and 3 (CMK-1 and 3) for hydrodesulphurization (HDS) of thiophene at specific conditions was explored to investigate the effect of different pore sizes, surface functional groups, metal dispersion, and presulfidation temperature. Co/CMK catalysts were superior to Mo/CMK catalysts on the basis of same metal loading. The synergistic effect was found at Co/Mo ratio of 5/5. Sulfidation on carbon supported catalysts was favored at lower temperature of 300 °C, whereas higher temperature of 400 and 500 °C showed a more favorable effect on alumina supported catalysts. CMK-3 supported CoMo catalysts were superior to all other catalysts due to larger pore size and higher acidic surface functional groups. CMK-3 oxidized with nitric acid showed even better performance for CoMo (5:5) supported catalysts since the increased surface functional groups might induce better dispersion leading to higher HDS activity.

1. Introduction

Hydrodesulfurization (HDS) has become a key process of refinery due to the implementation of more stringent specifications in sulfur content for diesel oil and gasoline toward cleaner fuels.[1] Sulfides of transition metals (Mo, W, Co, or Ni) are of great current industrial interest as catalysts in petroleum refining for hydroprocessing applications like HDS.[2] Since the beginning of the 20th century, these metals have been mostly used for HDS catalysis; no alternative to them has been reported.[3] Alumina is the most widely used support for the hydrotreating catalysts. But strong interaction of metal with alumina is undesirable as it gives a negative effect on the HDS activity. The quest for superior support system that avoids the main disadvantages of alumina has led researchers to explore alternative support materials.[4]

The discovery of first ordered mesoporous molecular sieves has sparked interest throughout the scientific community.[5] These sieves, discovered by Mobil researchers, have a high surface area (SA), pore volume (PV), and a narrow pore size distribution (PSD). Because of these charming properties, these materials got their place in heterogeneous catalysis as support for HDS catalysts. In spite of these excellent properties, practical applications of these materials are severely inhibited by their low hydrothermal stability and weak acidity.

Carbon has many positive attributes linked with it such as a high SA, availability of a large variety of PSDs, variable surface functional groups, and reduced coking propensity.[2,6] Carbon offers tremendous promise as a catalytic support material.[2] In recent years, carbon has received much attention as a support for HDS catalysts since high HDS activities have been reported which may originate from more favorable support/catalytic species interaction.[7] The catalytic activity for HDS of thiophene using supported metal sulfides increases in the order alumina < silica < carbon.[8] The use of carbon as a support for HDS catalysts has been studied by some researchers.[2,7,9−13] Utilized carbons are normally microporous with disordered pore structure and low specific PV, whereas catalytic processes for bulkier organic molecules (e.g., HDS) require supports with much larger and less tortuous pores than the microporous carbon supports.

The Ryoo group described the use of mesoporous silica as porous solid templates for the synthesis of a series of new ordered mesoporous carbons.[14−17] These ordered mesoporous carbons show great potential advantages over ordinary activated carbons (ACs) and silica supports[18] including large SA, high porosity, controlled narrow PSDs in the mesopore range, high thermal stability, high stability in strong acids and bases, high mechanical stability, and electric conductivity. Mesoporous carbon materials are of great interest for applications like adsorption,[19] host−guest chemistry,[20] electrochemical capacitance,[21] methane gas storage,[22] and in catalysis like liquid phase hydrogenation reactions[18] and methanol decomposition.[23]

Two types of mesoporous carbons were synthesized from two types of silica templates in this investigation. This study uses these new mesoporous carbons as a support for sulfided Mo, Co, and CoMo catalysts due to weak support−metal interaction.[7,24] Hence, one may have a better chance to study the roles of active metals. HDS activities of mesoporous carbons based Mo, Co, and CoMo catalysts are compared with commercial AC and alumina based catalysts to investigate the effect of characteristics of mesoporous carbon supports on catalytic activity and product selectivity. Mesoporous carbon was surface-modified to enhance surface functional groups and compared with other supports to find the appropriate best catalytic support.

2. Experimental Details

2.1. Synthesis of Supports and Surface Modification. Carbon mesostructures by KAIST-1 and 3 (CMK-1 and 3) were synthesized with different silica templates Mobil composition of matter-48 (MCM-48) and Santa Barbara amorphous-15 (SBA-15), respectively, using sucrose as a carbon precursor.[14,16,25] After carbonization in furnace at 900 °C under vacuum, silica

* To whom correspondence should be addressed. Tel.: +82-42-350-3915/3955. Fax: +82-42-350-5955. E-mail address: skihm@kaist.ac.kr.
† Korea Advanced Institute of Science and Technology.
‡ Current affiliation: Department of Chemical Engineering, COMSATS Institute of Information Technology Lahore Campus (CIIT Lahore), M.A. Jinnah Building, Defense Road, Off Raiwind Road, Lahore, Pakistan.

10.1021/ie801229y CCC: $40.75
Published on Web 12/05/2008

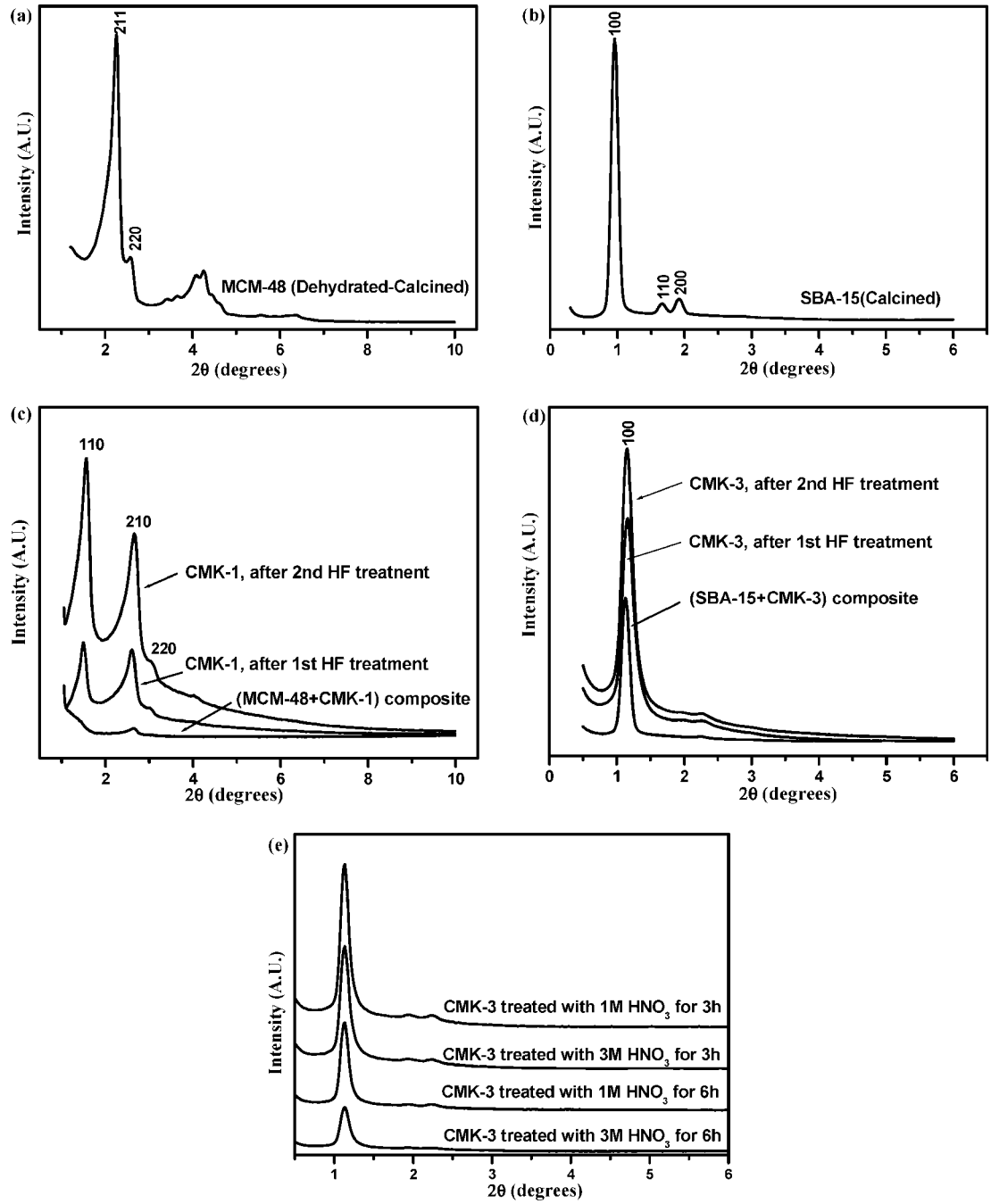

Figure 1. XRD patterns of (a) mesoporous silica template MCM-48, (b) mesoporous silica template SBA-15, (c) mesoporous carbon CMK-1, (d) mesoporous carbon CMK-3, and (e) surface-modified CMK-3.

Table 1. Carbon/Oxygen Formation Comparison and Silica Template Removal Confirmation by EDS Analysis

samples	C (%)	O (%)	Si (%)	S (%)
CMK-1 (synthesized, virgin)	96.00	3.81	0.06	0.12
CMK-3 (synthesized, virgin)	95.70	4.19	0.01	0.11
1 M HNO_3 treated CMK-3 (3 h)	92.80	7.58	0.04	0.13
3 M HNO_3 treated CMK-3 (3 h)	90.10	9.69	0.02	0.15

templates MCM-48 and SBA-15 were removed by dissolving with 10 and 5 wt % hydrofluoric acid (HF: 48−51%, J.T. Baker), respectively. The final mesoporous carbon products were dried at 100 °C.

CMK-3 and AC were oxidized with nitric acid to enhance oxygen containing functional groups on the carbon surface.[26,27] Different nitric acid concentrations (1 and 3 M) and times (3 and 6 h) at 60 °C were used for oxidizing 0.1 g of carbon sample with 10 mL of nitric acid solution. Subsequently, the carbon was filtered off, washed with distilled water, and dried at 100 °C in an inert atmosphere.

2.2. Catalyst Preparations. Equal numbers of metal atoms of Mo and Co were loaded with different weight percent (Mo 1.0, 3.4, 6.8, 10.0, and 14.8 equivalent to Co 0.6, 2.1, 4.2, 6.0, and 9.6) with ammonium heptamolybdate tetrahydrate (99.98%, Aldrich) and cobalt nitrate tetrahydrate (Aldrich) by incipient wetness. For CoMo catalysts, 6.261×10^{20} metal atoms/g cat (Mo 10 wt % or Co 6 wt %) were fixed and catalysts with different Co:Mo ratios (0:10, 3:7, 5:5, 7:3, and 10:0) were synthesized to find synergistic effect. CMK-1, CMK-3, AC, γ-Al_2O_3, oxidized CMK-3, and oxidized AC were used as support materials for Mo, Co, and CoMo catalysts. All the catalysts were dried at 100 °C.

Table 2. Physical Properties of Supports and Catalysts (Mo/CMK Catalysts[30])

CMK-1 Supported Mo, Co, or CoMo Catalysts				CMK-3 Supported Mo, Co, or CoMo Catalysts			
catalysts	S_{BET} (m^2/g)	PV (cm^3/g)	APD (nm)	catalysts	S_{BET} (m^2/g)	PV (cm^3/g)	APD (nm)
CMK-1	1690	1.39	3.0	CMK-3	1240	1.28	3.7
Mo(1.0)/CMK-1	1460	1.32	3.1	Mo(1)/CMK-3	1040	1.18	3.8
Mo(3.4)/CMK-1	1330	1.21	3.2	Mo(3.4)/CMK-3	764	1.02	3.7
Mo(10.0)/CMK-1	1070	1.04	3.2	Mo(10.0)/CMK-3	764	0.79	3.9
Mo(10.0)/CMK-1[a]	898	0.91	3.2	Mo(10.0)/CMK-3[a]	590	0.68	3.9
Co(0.6)/CMK-1	1540	1.35	3.2	Co(0.6)/CMK-3	1100	1.19	3.7
Co(2.1)/CMK-1	1390	1.24	3.2	Co(2.1)/CMK-3	920	0.98	3.8
Co(6.0)/CMK-1	1120	1.02	3.2	Co(6.0)/CMK-3	682	0.69	3.9
Co(6.0)/CMK-1[a]	967	0.92	3.2	Co(6.0)/CMK-3[a]	552	0.61	3.9
CoMo(0:10)/CMK-1	1070	1.04	3.2	CoMo(0:10)/CMK-3	764	0.79	3.9
CoMo(5:5)/CMK-1	1140	1.10	3.1	CoMo(5:5)/CMK-3	751	0.78	3.7
CoMo(10:0)/CMK-1	1120	1.02	3.2	CoMo(10:0)/CMK-3	682	0.69	3.9
CoMo(5:5)/CMK-1[a]	1010	1.01	3.2	CoMo(5:5)/CMK-3[a]	631	0.70	3.8
CMK-3 modification (1 M HNO_3 treatment)				CMK-3 modification (3 M HNO_3 treatment)			
CMK-3 (3 h)	1150	1.24	3.6	CMK-3 (3 h)	1100	1.15	3.5
CMK-3 (6 h)	1110	1.16	3.5	CMK-3 (6 h)	1080	1.11	3.5
CoMo(5:5)/CMK-3 (3 h)	645	0.72	3.6	CoMo(5:5)/CMK-3 (3 h)	602	0.65	3.6

[a] Used catalysts.

2.3. Characterization. The powder X-ray diffraction (XRD) patterns were recorded on a Rigaku Miniflex diffractometer with Cu Kα radiation at 40 kV and 45 mA. The Brunauer−Emmett−Teller surface area (S_{BET}), PV, and PSD of the supports were measured by the nitrogen adsorption−desorption method (ASAP 2000, Micromeritics). Information about the nature of the surface oxygen functional groups was obtained with a Fourier transform infrared (FT-IR) spectroscopy. Spectra were recorded on FT-IR spectrometer (Nexus, Nicolet) equipped with mercury cadmium telluride (MCT) detector with a resolution of 4 cm^{-1} and 200 scans per spectrum. Identification of surface oxygen groups was performed by neutralization with excess amount of various bases, followed by back-titration with hydrochloric acid.[28] The pH of the solutions of the carbon samples was measured by following the reported preocedure.[28] Philips CM200 instrument with 200 kV of acceleration voltage was used for transmission electron microscopy (TEM) test. CO chemisorption was performed by a dynamic method in once-through flow apparatus (Pulse Chemisorb 2705, Micromeritics) equipped with a thermal conductivity detector (TCD). A pulse of CO gas was introduced at 30 °C from a 6-port valve at an interval of 1 min. When the peaks attained a nearly constant area, the adsorption was assumed to reach saturation, and dispersion was calculated.

2.4. HDS Reaction. Thiophene HDS reaction was carried out at 400 °C in a stainless steel microflow reactor operated at 20 atm pressure. The liquid thiophene flow rate was 0.035 mL/min, the mole ratio of hydrogen to thiophene was 15, and *W*/*F* (weight of catalyst/thiophene flow rate; space time) was 5.71 g cat min/mL thiophene. Before starting the reaction, each catalyst was calcined and sulfided in situ at 300 or 400 °C for 2 h with a flow of H_2S (10 vol %)/H_2 mixture at 30 mL/min. Reaction products were analyzed by using a gas chromatograph (Hewlett-Packard, 5710A) equipped with TCD and packed column.

3. Results and Discussion

3.1. Mesostructure of CMK-1 and CMK-3. The obtained mesoporous carbon CMK-1, from MCM-48 template, exhibited XRD pattern with several sharp low-angle reflections (Figure 1 part c) and showed a somewhat different pattern than MCM-48 (Figure 1 part a). Carbon structures formed in the porous silica template having two disconnected systems are also disconnected and are capable of changing their positions with respect to one another when the template is removed.[29] After the removal of the silica template, CMK-1 showed an additional relatively narrow (110) diffraction line in its diffraction pattern, confirming that MCM-48 is transformed into another structure with somewhat lower symmetry. This indicates that the topology has changed and that CMK-1 is not a true replica of MCM-48. Large 2D hexagonal mesoporous channels of SBA-15 are interconnected through spacers. The structure of CMK-3 is also composed of 2D hexagonal mesoporous carbon rods. The carbon nanorods are interconnected by spacers, which are constituted by the carbon that filled the channel interconnecting micropores within the SBA-15 wall.[17] CMK-3 showed a well resolved XRD peak of 2D hexagonal space group (p6 mm) (Figure 1 part d), similar to the case of SBA-15 (Figure 1 part b). CMK-3 carbon is negative replica of the mesoporous silica template SBA-15. Figure 1 (part e) showed the XRD patterns of CMK-3 after nitric acid treatment for enhancing surface functional groups. There was a small decrease in the characteristic peaks of CMK-3 by increasing the nitric acid concentration from 1 to 3 M. A significant decrease in XRD peaks was observed by treating CMK-3 for long time (6 h). Long time nitric acid treatment can destroy the surface as well as the internal pore structure of the carbon,[27] which causes a decrease in peaks. The peaks showed that CMK-3 carbon maintained the structure even after the severe nitric acid treatment. The structure stability of CMK-3 carbon is high and showed a good resistance against erosive effect of nitric acid.

Energy dispersive spectroscopy (EDS) analysis (Table 1) confirmed the synthesis of mesoporous carbon supports CMK-1 and CMK-3 which were almost pure carbon materials and silica templates were almost completely dissolved by HF. CMK-3 oxidized with nitric acid showed a decrease in C % and an increase in O % with increasing acid concentration, which indicates an increase in surface oxi functional groups.

3.2. Metal-Supported CMK-1 and CMK-3. CMK-1 and CMK-3 showed high S_{BET}, PV, and confined average pore diameter (APD) (Table 2) values. CMK-3 showed a larger pore size of 3.7 nm compared to CMK-1 that showed 3.0 nm. A decrease in the physical characteristic of supports is shown after Mo,[30] Co, and CoMo metal impregnation because of increased density by depositing metals and partially from pore blockage by these metal species. A further small decrease was observed in these characteristics in used catalysts. Table 2 shows the physical properties of CMK-3 after nitric acid treatment. There was a small decrease in SA and PV by increasing the acid

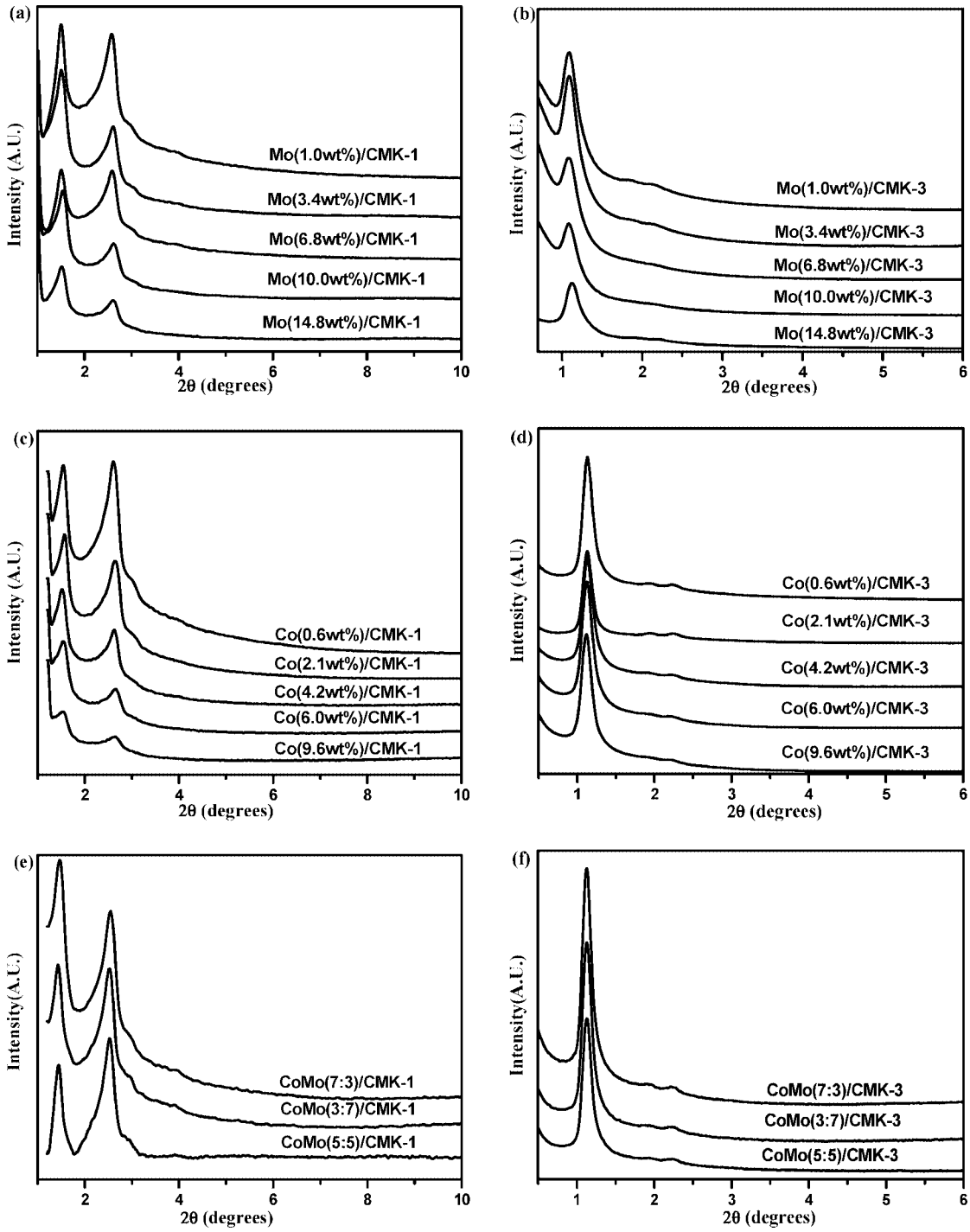

Figure 2. XRD patterns of (a) Mo(x)/CMK-1,[30] (b) Mo(x)/CMK-3,[30] (c) Co(x)/CMK-1, (d) Co(x)/CMK-3, (e) CoMo(x)/CMK-1, and (f) CoMo(x)/CMK-3 catalysts.

concentration and treatment time. This might be due to increased additional mass after acid treatment. The higher acid concentration for long treatment may also damage the internal pore structure of carbon due to the incorporation of oxygen functionalities in pore walls and the erosive effect of nitric acid.[27]

Figure 2 represents the XRD results of CMK-1 and CMK-3 carbon supported Mo,[30] Co, and CoMo catalysts. A small but gradual decrease was observed in the main XRD peaks of CMK-1 and CMK-3 supports due to metal impregnation. The supports retained their mesoporosity and crystallinity as observed from the main XRD peak intensities of the supports even after metal impregnation. This means that structural order was still maintained even after metal impregnation. However, the diffraction intensity weakened as the metal content increased, indicating that the encapsulation of metal composites decreased the order in the mesostructure. These results correlate with BET results (Table 2).

3.3. Surface Functional Groups. Suh et al.[28] and Vissers et al.[12] indicated that surface oxygen functional groups could affect carbon−metal interaction and catalytic activity of carbon-supported catalysts. Oxygen surface functional groups were responsible for the strength and extent of the interaction between metal and the carbon surface. The surface chemistry of carbon is explored in this study (Figure 3 and Table 3), to find the

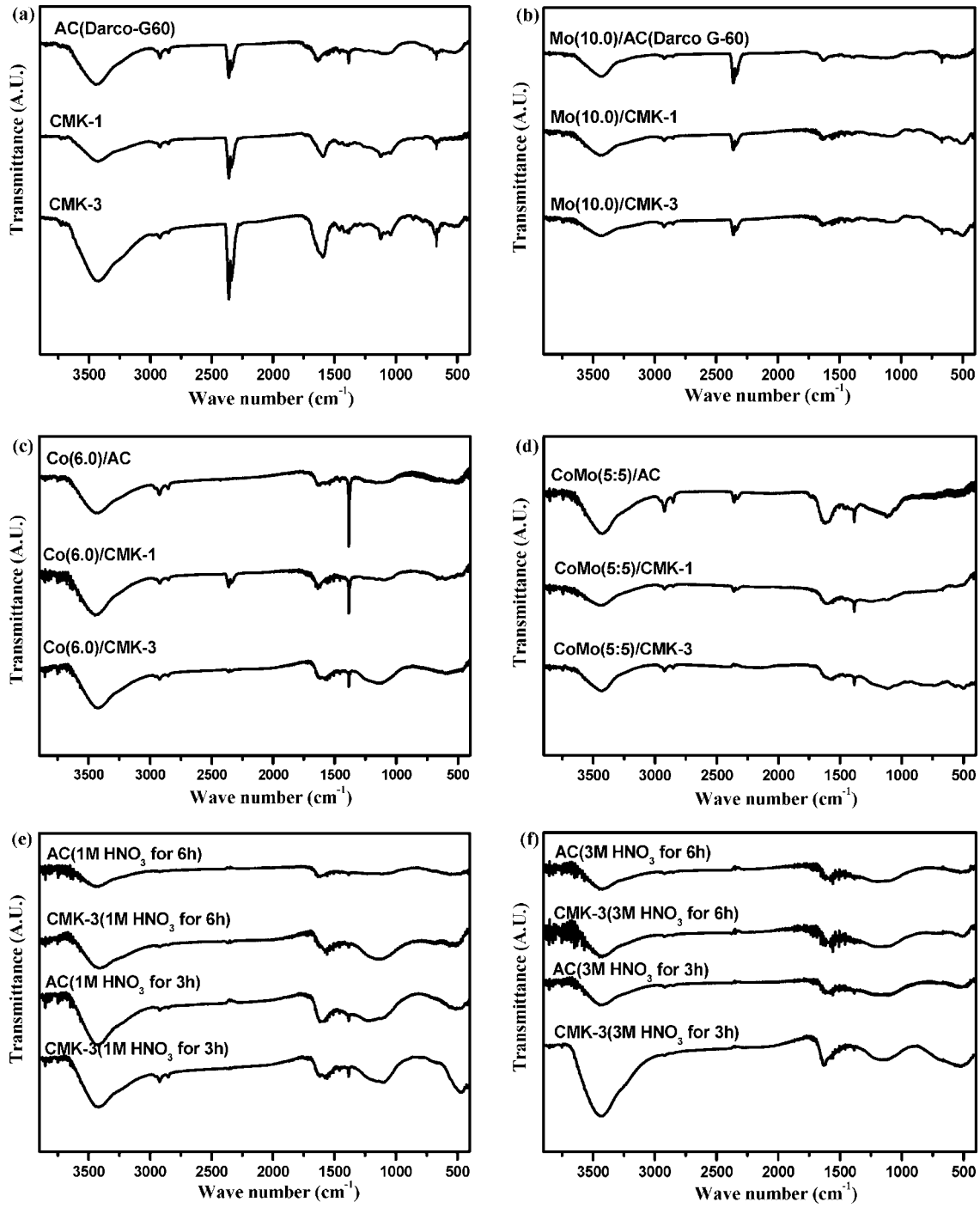

Figure 3. FT-IR transmittance spectra for surface functional groups: (a) carbon supports,[30] (b) carbon supported Mo(10.0) catalysts,[30] (c) carbon supported Co(6.0) catalysts, (d) carbon supported CoMo(5:5) catalysts, (e) CMK-3 and AC treated with 1 M HNO_3, and (f) CMK-3 and AC treated with 3 M HNO_3.

qualitative and quantitative acidic and basic oxygen functional groups and pH of the solution of these supports.

FT-IR reflectance spectra of the carbon supports and their supported Mo, Co, and CoMo catalysts are shown in Figure 3 (parts a−d). FT-IR spectra of the supports (Figure 3 part a) show characteristic bands at wave numbers ranging from 500 to 930 cm^{-1}, which are attributed to C−H vibrations.[31] The bands appear at an intensity of 1030 to 1120 cm^{-1} are assigned to OH bendings, whereas 1255 to 1320 cm^{-1} are the bands for C−O−C stretching, alcoholic, phenolic, and carboxylic groups. The band around 1590 cm^{-1} is due to olefinic C═C bonds, and the band around 3500 cm^{-1} is due to OH groups. CMK-3 has more oxygen surface functional groups compared to CMK-1 and AC (Figure 3 part a). A significant decrease in the band intensities is observed because of the metal dispersion on the supports (Figure 3 parts b−d). Figure 3 (parts e and f) shows oxidized CMK-3 which contains higher surface functional groups than oxidized AC. Surface functional groups in CMK-3 increased with increasing acid concentration and decreasing treatment time, while a decrease in surface functional groups occurred with increase in both acid concentration and treatment time for AC. The oxidized CMK-3 (3 M, 3 h) and AC (1 M, 3 h) show a broad band at 1500 to 1700 cm^{-1} and a broad envelope from 1000 to 1400 cm^{-1}. The latter can be mainly attributed to carboxylic groups created by oxidative treatment, while the broad band from 1500−1700 cm^{-1} is assigned to the

Table 3. Surface Functional Groups Measurement by Acid−Base Titrations

sample	pH	total basic groups (mmol/g)	detailed acidic functional groups: carboxylic (mmol/g) $NaHCO_3$	detailed acidic functional groups: lactonic (mmol/g) Na_2CO_3	detailed acidic functional groups: phenolic (mmol/g) NaOH	total acidic groups (mmol/g)
CMK-1 (virgin)	5.8	0.25	0.435	0.261	0.382	1.08
CMK-3 (virgin)	5.5	0.24	0.531	0.258	0.422	1.21
AC (virgin)	6.2	0.36	0.351	0.112	0.327	0.79
CMK-3 (1 M, 3 h)	5.2	0.18	0.783	0.241	0.650	1.67
CMK-3 (3 M, 3 h)	4.9	0.10	0.825	0.253	0.901	1.98
CMK-3 (1 M, 6 h)	5.4	0.20	0.651	0.301	0.490	1.44
CMK-3 (3 M, 6 h)	5.5	0.20	0.520	0.412	0.415	1.35
AC (1 M, 3 h)	5.7	0.27	0.550	0.135	0.592	1.28
AC (3 M, 3 h)	5.8	0.20	0.490	0.120	0.481	1.09
AC (1 M, 6 h)	6.0	0.25	0.381	0.252	0.351	0.98
AC (3 M, 6 h)	6.1	0.31	0.330	0.290	0.302	0.92

C═O stretching frequency of the COOH groups or to an aromatic ring-stretching mode.[28] The big band around 3400 cm^{-1} is due to OH groups present on the carbon surface. Here, the increase in the intensity of the bands may be associated with an increase of surface acidic functional groups by the oxidative treatment.

Table 3 shows the quantitative amount of acidic as well as basic oxygen surface functional groups measured by acid−base titration. CMK-3 shows the higher acidic surface functional groups compared to CMK-1 and AC in the form of carboxylic, lactonic, and phenolic groups measured by $NaHCO_3$, Na_2CO_3, and NaOH, respectively. The pH measurement results of the carbon samples also support the functional group analysis results (Table 3). Oxidized CMK-3 (3 M, 3 h) shows the highest surface functional groups compared to other conditions and also from AC at all conditions. There is a significant increase in the carboxylic and phenolic groups with increase of acid concentration and an increase in the lactonic group with the increase of treatment time. At the same time, as acidic groups increase there is a decrease in basic functional groups, which is further confirmed by pH measurements. These results correlate with the FT-IR (Figure 3) and EDS (Table 1) results.

3.4. HDS Activity. Thiophene HDS activity for supported Mo and Co catalysts with different metal loading was performed at specific reaction conditions (presulfiding at 300 and 400 °C, pressure 20 atm, reaction temperature 400 °C, reaction time 7 h, H_2/thiophene 15). Among those, Mo (10 wt %) and Co (6 wt %) loadings presulfided at 300 °C showed the highest catalytic activity (Figure 4). Farag et al.[2] reported the influence of metal

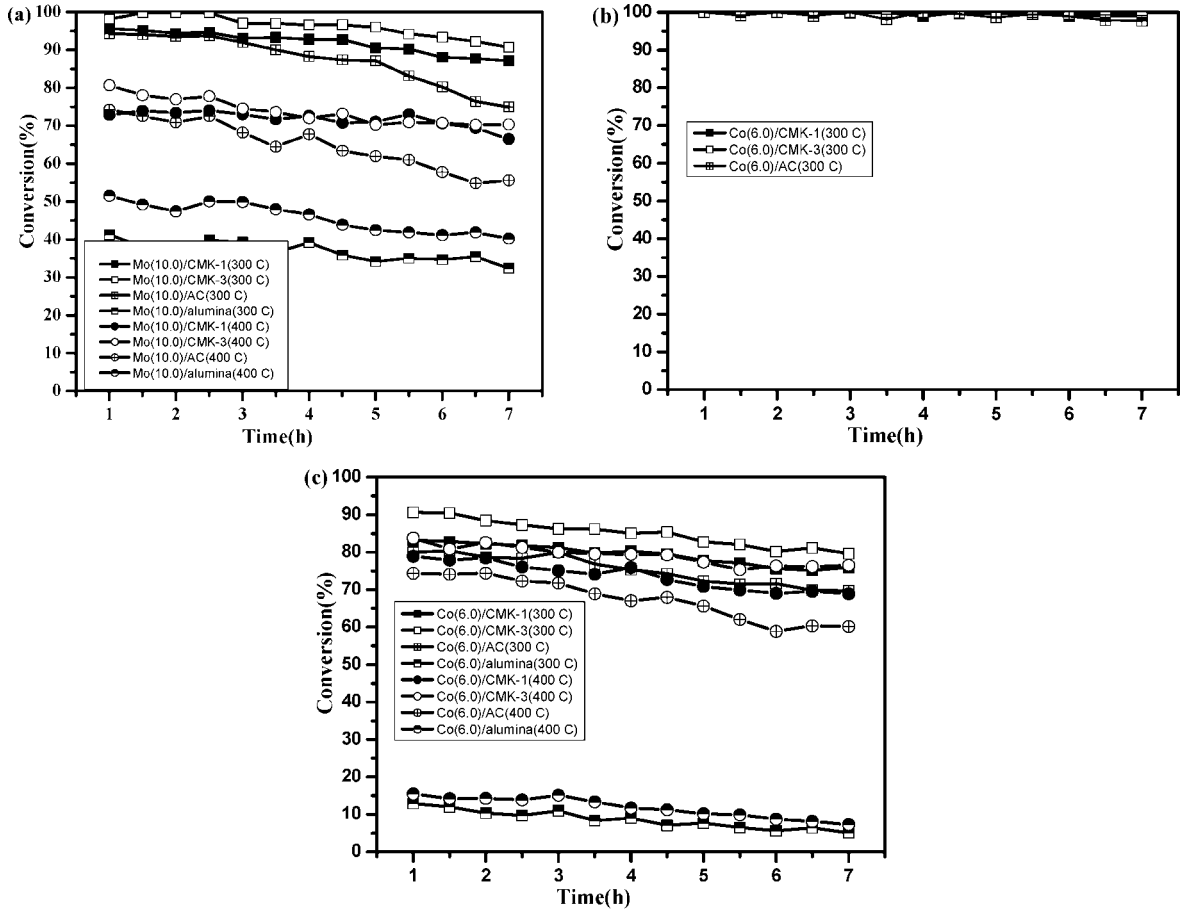

Figure 4. Thiophene HDS activity over supported (a) Mo catalysts,[30] (b) Co catalysts at low thiophene flow rate, and (c) Co catalysts at high thiophene flow rate.

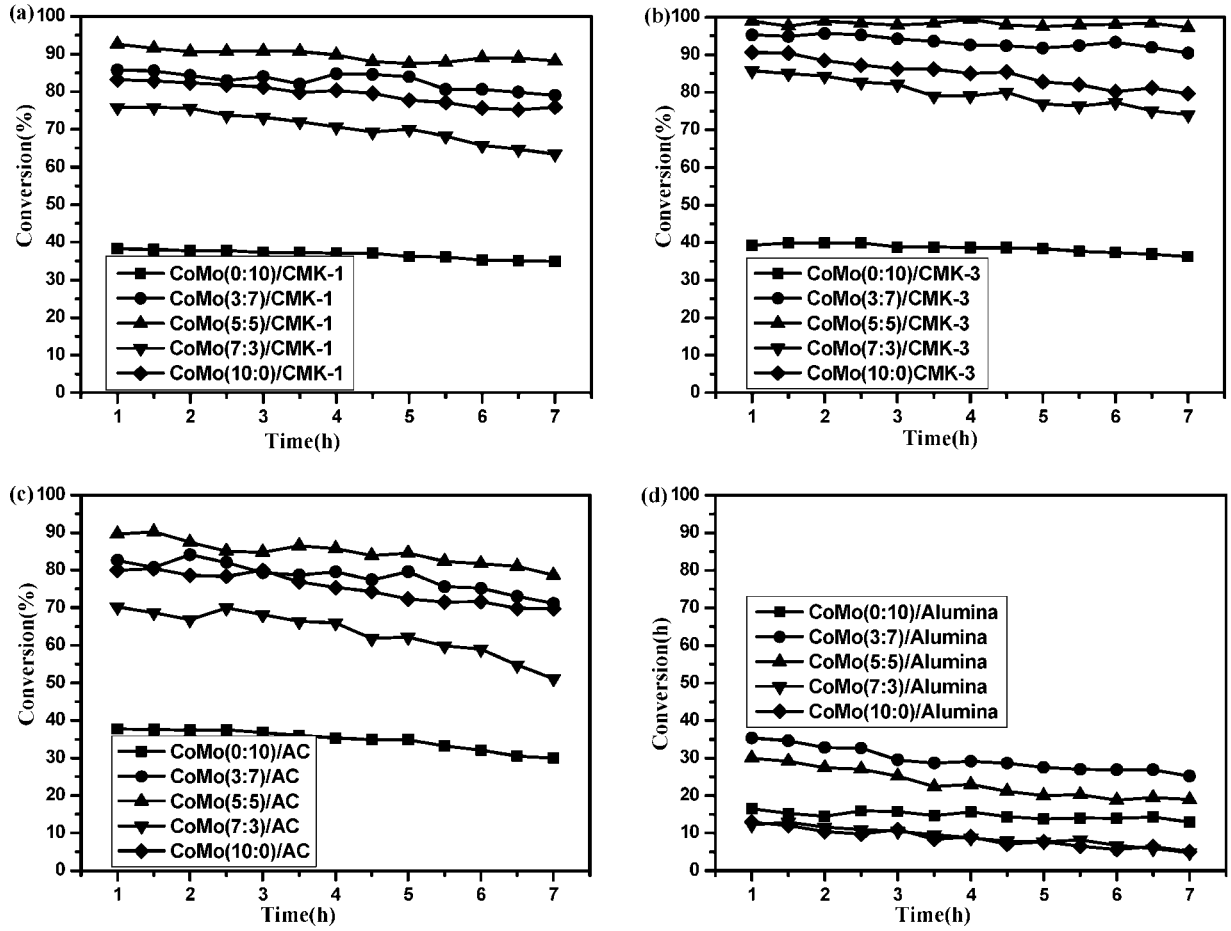

Figure 5. Synergistic effect between Co and Mo in (a) CoMo/CMK-1, (b) CoMo/CMK-3, (c) CoMo/AC, and (d) CoMo/alumina catalysts for thiophene HDS with time on stream.

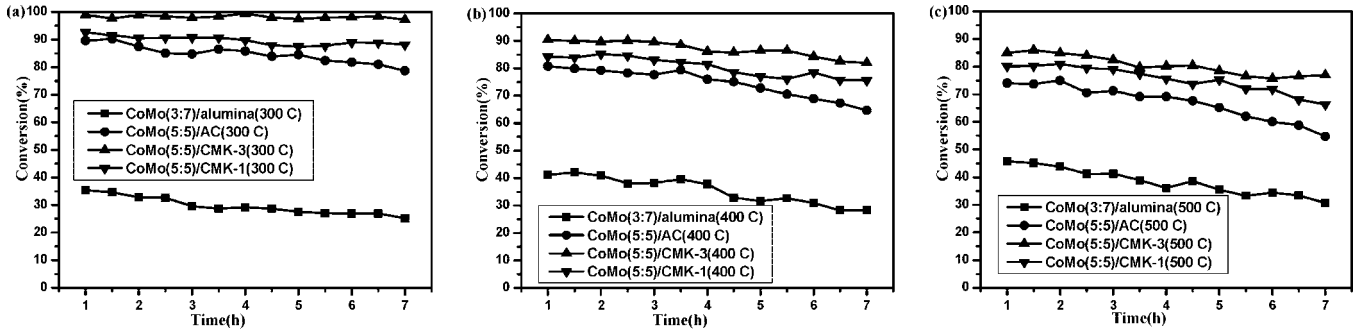

Figure 6. Effect of the catalyst presulfidation temperature (a) 300, (b) 400, and (c) 500 °C on thiophene HDS activity over CoMo(5:5)/(CMK-1 or CMK-3 or AC or alumina) catalysts with time on stream.

presulfidation on the catalytic properties of carbon supported catalysts. Sintering of the active phase was observed during sulfiding the Mo/C catalysts, indicating a certain mobility of the Mo phase during sulfiding. The results showed that the agglomeration of Mo phases was noted at a high concentration of Mo at higher temperature. Therefore, a lower presulfidation temperature is a best option for CMK supported Mo or Co catalysts to achieve the best performance. A significant increase in thiophene activity was observed by presulfiding the CMK and AC supported Mo/Co catalysts at 300 °C instead of at 400 °C, whereas an opposite response was seen with Al_2O_3 supported catalysts (Figure 4 parts a and c). CMK-3 supported catalysts showed the highest activity among all other (CMK-1, AC, and Al_2O_3) supported catalysts (Figure 4) due to the larger mesopore size of 3.7 nm (Table 2) and higher acidic surface functional groups (Table 3). The larger mesopores of CMK-3 support with higher acidic surface functional groups, acted as transport pores, which facilitated the metal dispersion and transportation of the reactant and product molecules to reach the smaller pores situated in the interior of the carbon particles. Furthermore, Co/(CMK or AC) supported catalysts were superior to Mo/(CMK or AC) supported catalysts in HDS activity as evidenced in Figure 4 (parts a and b) with the same space time (5.71 g cat min/cm^3 thiophene). Higher space time (2.22 g cat min/cm^3 thiophene) reduced the catalytic conversion as shown in Figure 4 (part c). Figure 4 (part b) shows that the catalytic conversions with Co catalysts are almost complete. This indicates that Co was more effectively used on the carbon supports than on alumina support, indicating that Co might act as a catalyst instead of a promoter.

Table 4. Metal Dispersion by CO Chemisorption Analysis

catalysts (sulfided)	metal dispersion (%) by CO chemisorptions at 30 °C	
	catalysts sulfided at 300 °C	catalysts sulfided at 400 °C
Mo(10.0)/CMK-1	26	20
Mo(10.0)/CMK-3	32	25
Mo(10.0)/AC	20	14
Mo(10.0)/alumina	8	10
Co(6.0)/CMK-1	65	58
Co(6.0)/CMK-3	72	66
Co(6.0)/AC	57	49
Co(6.0)/alumina	5	7
CoMo(5:5)/CMK-1	58	51
CoMo(5:5)/CMK-3	67	59
CoMo(5:5)/AC	48	41
CoMo(3:7)/alumina	10	14
CoMo(5:5)/CMK-3 (1 M, 3 h)	75	
CoMo(5:5)/CMK-3 (3 M, 3 h)	84	
CoMo(5:5)/AC (1 M, 3 h)	64	
CoMo(5:5)/AC (3 M, 3 h)	55	

The synergistic effect in the HDS activity of the industrially used sulfides Co−Mo−S_X, Ni−Mo−S_X, Ni−W−S_X, and also of the related system Co−W−S_X, is very pronounced, the mixed catalysts being several times more active than the individual components. The effect is easily observable on both supported and unsupported systems, independent of the method of preparation and the procedure used for the evaluation of activity.[32] Figure 5 (parts a−c) showed the synergistic effect between Co and Mo supported on CMK-1, CMK-3, and AC (presulfiding at 300 °C, pressure 20 atm, reaction temperature 400 °C, reaction time 7 h, H_2/thiophene 15, *W*/*F* 2.22 g cat min/cm^3 thiophene). The highest activity (synergism between

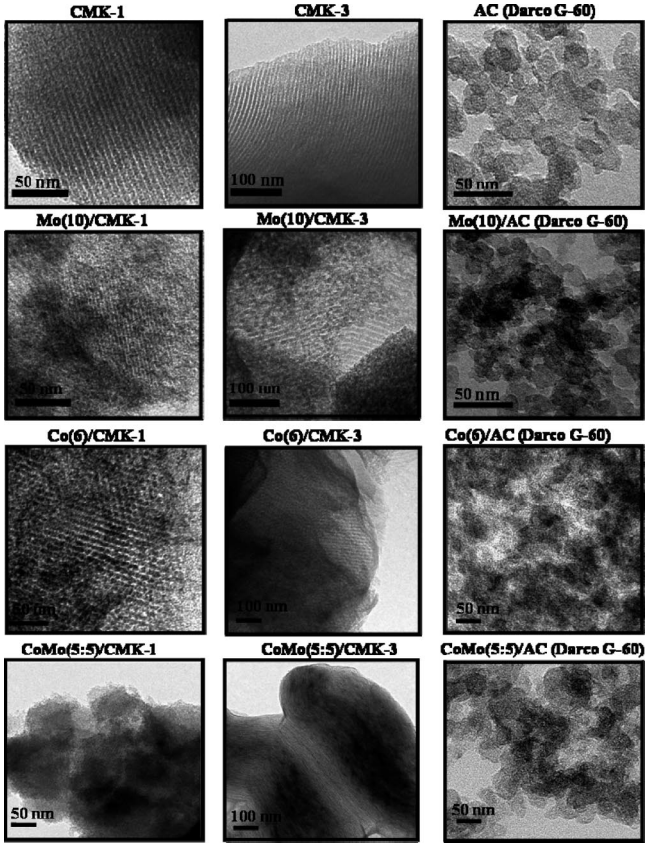

Figure 7. TEM images of CMK-1, CMK-3, AC supports, and their supported sulfided Mo,[30] Co, and CoMo catalysts showing metal distribution.

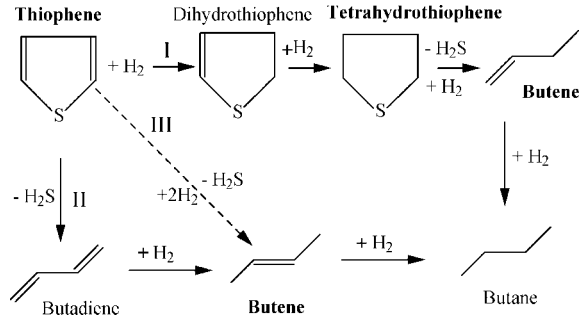

Figure 8. HDS reaction path network of thiophene.

Co and Mo) was observed at Co/Mo ratio of 5/5. CoMo(5:5)/CMK-3 catalysts showed the highest catalytic performance, even higher than Co/CMK catalysts.

CoMo/alumina showed a synergistic effect at Co/Mo ratio of 3/7 due to strong metal−support characteristic. The activity of CoMo/alumina catalysts is also comparatively much lower than CoMo/(CMK, AC) catalysts. The strong chemical interaction of metals with alumina support nullifies the activity of expensive metal species compared to carbon supports which have weak metal−support interaction.[24]

3.5. Presulfidation Temperature Effect. The presulfidation temperature effect in supported CoMo catalysts was very clearly shown in Figure 6, when the catalysts were presulfided at 300, 400, and 500 °C (pressure 20 atm, reaction temperature 400 °C, reaction time 7 h, H_2/thiophene 15, *W*/*F* 2.22 g cat min/cm^3 thiophene). A low presulfidation temperature is favorable as there is weak interaction between metal and carbon support. At higher presulfidation temperatures, the chance of sintering is very high because of the large mobility of metal (weak metal−carbon interaction). This supports the results in this study where the highest activity was observed when catalysts were presulfded at 300 °C and the lowest when the catalysts have presulfidation temperature of 500 °C in case of carbon supported catalysts. However, opposite observations were made with alumina support.

3.6. Metal Dispersion and Distribution. Table 4 shows the metal dispersion by CO chemisorption at 30 °C of supported sulfided Mo, Co, and CoMo catalysts presulfided at 300 and 400 °C. The catalyst presulfided at 300 °C showed higher metal dispersion compared to the catalyst presulfided at 400 °C. Co supported catalysts showed the higher dispersion than their equivalent Mo supported catalysts, which correlates with the reaction results (Figure 4). Also, CMK-3 supported Mo, Co, and CoMo catalysts showed higher dispersion than CMK-1 and AC supported catalysts because of larger pore size and higher surface functional groups on its surface.

TEM images of CMK-1 and CMK-3 ordered mesostructures, and AC disordered structure are shown in Figure 7. CMK-1 or CMK-3 supported Mo, Co, and CoMo catalysts showed uniform distribution of metals, whereas in case of AC supported Mo, Co, and CoMo catalysts metal clusters were clearly observed due to metal agglomeration.

3.7. Product Selectivity. The HDS reaction path network of thiophene is shown in Figure 8. HDS of thiophene mainly takes place in three pathways: HDS via hydrogenation followed by desulfurization (hydrogenation pathway I), C−S bond scission (hydrogenolysis pathway II), or direct desulfurization (direct pathway III).

According to selectivity results in Figure 9 (presulfiding at 300 °C, pressure 20 atm, reaction temperature 400 °C, reaction time 7 h, H_2/thiophene 15, *W*/*F* 2.22 g cat min/cm^3 thiophene),

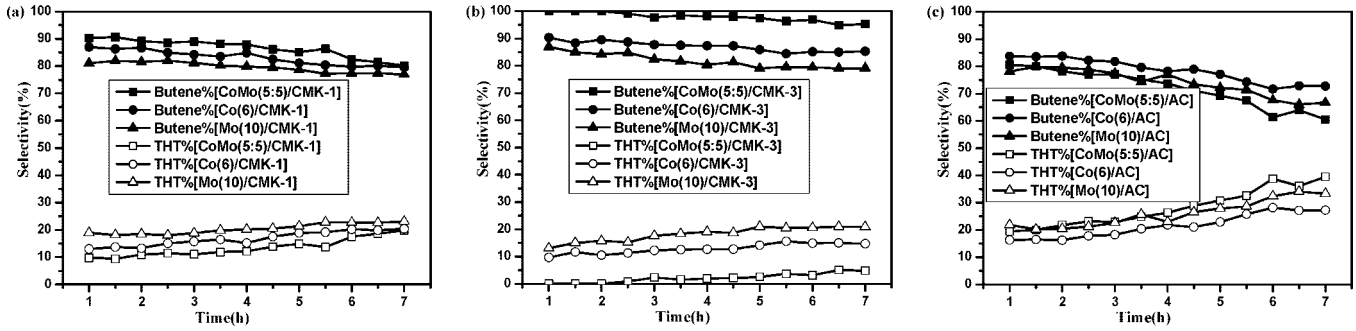

Figure 9. Thiophene HDS selectivity for Mo(10.0),[30] Co(6.0), and CoMo(5:5) catalysts supported over (a) CMK-1, (b) CMK-3, and (c) AC.

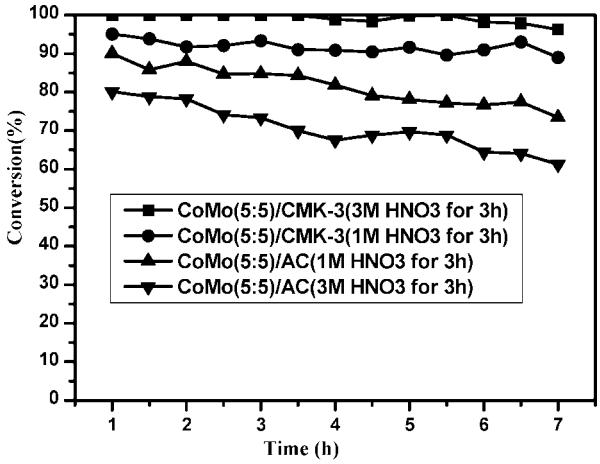

Figure 10. Thiophene HDS activity over modified carbon supported CoMo catalysts with time on stream.

AC supported Mo, Co, and CoMo catalysts showed more tetrahydrothiophene (pathway I), whereas in case of CMK-1 and CMK-3 supported catalysts, more butene was observed (pathways II or III). A greater number of acidic surface functional groups on CMK-1 and CMK-3 favored the direct desulfurization pathway as compared to AC which had fewer such groups. HDS selectivity decreased in the order as follows: CoMo/carbon > Co/carbon > Mo/carbon.

3.8. CMK-3 Modification Effect on HDS Activity. Thiophene HDS activity over modified CMK-3 and AC supported CoMo(5:5) catalysts with time on stream at specific reaction conditions (presulfidation temperature 300 °C, reaction temperature 400 °C, pressure 20 atm, reaction time 7 h, H_2/thiophene 15, *W/F* 1.90 g cat min/cm^3 thiophene) is shown in Figure 10. CoMo(5:5)/CMK-3 (3 M, 3 h) showed the highest activity, while the CoMo(5:5)/AC (3 M, 3 h) showed the lowest. It might be due to the higher surface functional groups on the surface of CMK-3 (3 M, 3 h) compared to the other cases as shown (Table 3). These surface functional groups caused higher metal dispersion (Table 4). The more acidic groups, basically carboxylic in nature, are expected to have a major influence on the metal dispersion.[28] Therefore, these acidic surface oxygen functional groups might increase the affinity of the carbon support for the metal precursor aqueous solution by enhancing the hydrophilicity of the carbon surface and finally led to more uniform distribution of the precursor throughout the internal pore structure which caused higher HDS activity.

4. Conclusions

MCM-48 and SBA-15 silica templates were synthesized to prepare mesoporous carbon supports CMK-1 and CMK-3, respectively. CMK supported sulfided Co catalysts showed superior performance due to higher metal dispersion to CMK supported sulfided Mo catalysts. The synergistic effect between Co and Mo (at Co/Mo ratio of 5/5) supported on CMK resulted in better HDS performance than with Co/CMK catalysts. CMK-3 supported sulfided Mo, Co, and CoMo catalysts have shown significantly better performance in terms of thiophene HDS activity and product selectivity compared to CMK-1, AC, and alumina supported catalysts. Surface modified CMK-3 supported CoMo (5:5) catalysts showed further better performance. The enhancement in activity was believed to be due to larger pore size, higher surface oxygen functional groups, higher metal dispersion, and better structure connectivity of CMK-3. These factors might increase the interaction between the support and metal precursor solution through enhanced hydrophilicity to give uniform and better metal distribution and dispersion, which facilitated the transport of reactant and product molecules to give better HDS activity. It was demonstrated in this work that surface modified mesoporous carbon with uniform mesopores could make promising support for HDS catalysts, compared to conventional AC or alumina supports.

Acknowledgment

Financial support by the grant of Brain Korea 21 (BK21) Project and partially by the National Research Laboratory Project of Korea Ministry of Science and Technology is gratefully acknowledged. M.H. is also thankful to Korea Research Foundation (KRF) for the scholarship.

Literature Cited

(1) Topsoe, H.; Clausen, B. S.; Massoth, F. E. *Hydrotreating Catalysis*; Springer: Berlin, 1996.

(2) Farag, H.; Whitehurst, D. D.; Mochida, I. Synthesis of Active Hydrodesulfurization Carbon-Supported Co-Mo Catalysts. Relationships between Preparation Methods and Activity/Selectivity. *Ind. Eng. Chem. Res.* **1998**, *37*, 3533.

(3) Afanasiev, P.; Bezverkhyy, I. Ternary Transition Metals Sulfides in Hydrotreating Catalysis. *Appl. Catal. A−Gen.* **2007**, *322*, 129.

(4) Hussain, M.; Song, S. K.; Lee, J. H.; Ihm, S. K. Characteristics of CoMo Catalysts Supported on Modified MCM-41 and MCM-48 Materials for Thiophene Hydrodesulfurization. *Ind. Eng. Chem. Res.* **2006**, *45*, 536.

(5) Kresge, C. T.; Leonowicz, M. E.; Roth, W. J.; Vartuli, J. C.; Beck, J. S. Ordered Mesoporous Molecular Sieves Synthesized by a Liquid-Crystal Temple Mechanism. *Nature.* **1992**, *359*, 710.

(6) de Oliveira, E. C.; Pires, C. T. G. V. M. T.; Pastore, H. O. Why Are Carbon Molecular Sieves Interesting. *J. Braz. Chem. Soc.* **2006**, *17*, 16.

(7) Farag, H.; Mochida, I.; Sakanishi, K. Fundamental Comparison Studies on Hydrodesulfurization of Dibenzothiophenes over CoMo-Based Carbon and Alumina Catalysts. *Appl. Catal. A−Gen.* **2000**, *194−195*, 147.

(8) Martín-Gullón, A.; Prado-Burguete, C.; Rodriguez-Reinoso, F. Effect of Carbon Properties on the Preparation and Activity of Carbon-Supported Molybdenum Sulfide Catalysts. *Carbon.* **1993**, *31*, 1099.

(9) Sakanishi, K.; Mochida, I.; Whitehurst, D. D. Hydrodesulfurization Kinetics and Mechanism of 4,6-dimethyldibenzothiophene over NiMo Catalyst Supported on Carbon. *J. Mol. Catal. A: Chem.* **2000**, *155*, 101.

(10) Shu, Y.; Oyama, S. T. Synthesis, Characterization, and Hydrotreating Activity of Carbon-Supported Transition Metal Phosphides. *Carbon.* **2005**, *43*, 1517.

(11) Moon, S. J.; Ihm, S. K. Nitric Oxide Chemisorption and Temperature-Programmed Desorption Study of Cobalt and Molybdenum Catalysts Supported on Activated Carbon and Alumina. *Appl. Catal.* **1988**, *42*, 307.

(12) Vissers, J. P. R.; de Beer, V. H. J.; Prins, R. The Role of Co in Sulphidised Co-Mo Hydrodesulfurization Catalysts Supported on Carbon and Alumina. *J. Chem. Soc., Faraday Trans 1* **1987**, *83*, 2145.

(13) Ferrari, M.; Delmon, B.; Grange, P. Influence of the Active Phase Loading in Carbon Supported Molybdenum-Cobalt Catalysts for Hydrodeoxygenation Reactions. *Carbon* **2002**, *40*, 497.

(14) Ryoo, R.; Joo, S. H.; Jun, S. Synthesis of Highly Ordered Carbon Molecular Sieves via Template-Mediated Structural Transformation. *J. Phys. Chem. B* **1999**, *103*, 7743.

(15) Joo, S. H.; Jun, S.; Ryoo, R. Synthesis of Ordered Mesoporous Carbon Molecular Sieves CMK-1. *Microporous Mesoporous Mater.* **2001**, *44*−*45*, 153.

(16) Kruk, M.; Jaroniec, M.; Ryoo, R.; Joo, S. H. Characterization of Ordered Mesoporous Carbons Synthesized using MCM-48 Silica as Templates. *J. Phys. Chem. B* **2000**, *104*, 7960.

(17) Solovyova, L. A.; Shamkov, A. N.; Zaikovskiib, V. I.; Joo, S. H.; Ryoo, R. Detailed Structure of the Hexagonally Packed Mesostructured Carbon Material CMK-3. *Carbon* **2002**, *40*, 2477.

(18) Ahn, W. S.; Min, K. I.; Chung, Y. M.; Rhee, H. K.; Joo, S. H.; Ryoo, R. Novel Mesoporous Carbon as a Catalyst Support for Pt and Pd for Liquid Phase Hydrogenation Reactions. *Stud. Surf. Sci. Catal.* **2001**, *135*, 313.

(19) Zhou, L.; Li, J.; Wang, N.; Wang, Z.; Zhou, Y. Synthesis of Ordered Mesoporous Carbon Molecular Sieve and its Adsorption Capacity for H_2, N_2, O_2, CH_4, and CO_2. *Chem. Phys. Lett.* **2005**, *413*, 6.

(20) Huwe, H.; Fröba, M. Iron (III) Oxide Nanoparticles within the Pore System of Mesoporous Carbon CMK-1: Intra-Pore Synthesis and Characterization. *Microporous Mesoporous Mater.* **2003**, *60*, 151.

(21) Zhou, H.; Zhu, S.; Hibino, M.; Honma, I. Electrochemical Capacitance of Self-Ordered Mesoporous Carbon. *J. Power Sources* **2003**, *122*, 219.

(22) Zhou, H.; Zhu, S.; Honma, I.; Seki, K. Methane Gas Storage in Self-Ordered Mesoporous Carbon (CMK-3). *Chem. Phys. Lett.* **2004**, *396*, 252.

(23) Minchev, C.; Tsoncheva, T.; Paneva, D.; Dimitrov, M.; Mitov, I.; Fröba, M. Iron Oxide Modified Mesoporous Carbons: Physicochemical and Catalytic Study. *Microporous Mesoporous Mater.* **2005**, *81*, 333.

(24) Lee, J. J.; Han, S.; Kim, H.; Koh, J. H.; Hyeon, T.; Moon, S. H. Performance of CoMoS Catalysts Supported on Nanoporous Carbon in the Hydrodesulfurization of Dibenzothiophene and 4,6-dimethyldibenzothiophene. *Catal. Today* **2003**, *86*, 141.

(25) Jun, S.; Joo, S. H.; Ryoo, R.; Kruk, M.; Jaroniec, M.; Liu, Z.; et al. Synthesis of New, Nanoporous Carbon with Hexagonally Ordered Mesostructure. *J. Am. Chem. Soc.* **2000**, *122*, 10712.

(26) Yin, C. Y.; Aroua, M. K.; Daud, W. M. A. W. Review of Modifications of Activated Carbon for Enhancing Contaminant Uptakes from Aqueous Solutions. *Sep. Purif. Technol.* **2007**, *52*, 403.

(27) Stavropoulos, G. G.; Samaras, P.; Sakellaropoulos, G. P. Effect of Activated Carbons Modification on Porosity, Surface Structure and Phenol Adsorption. *J. Hazard. Mater.* **2008**, *151*, 414.

(28) Suh, D. J.; Park, T. J.; Ihm, S. K. Effect of Surface Oxygen Groups of Carbon Supports on the Characteristics of Pd/C Catalysts. *Carbon* **1993**, *31*, 427.

(29) Ryoo, R.; Joo, S. H.; Kruk, M.; Jaroniec, M. Ordered Mesoporous Carbons. *Adv. Mater.* **2001**, *13*, 677.

(30) Hussain, M.; Ihm, S. K. Characteristics of Mesoporous Carbons Supported Mo Catalysts in Thiophene Hydrodesulfurization. *Stud. Surf. Sci. Catal.* **2007**, *170* (B), 1368.

(31) Kim, D. J.; Yie, J. E.; Kim, S. J.; Kim, J. M. Ordered Mesoporous Carbons: Implication of Surface Chemistry, Pore Structure and Adsorption of Methyl Mercaptan. *Carbon* **2005**, *43*, 1868.

(32) Zdrazil, M. Recent Advances in Catalysis over Sulphides. *Catal. Today* **1988**, *3*, 269.

Received for review August 11, 2008
Revised manuscript received September 29, 2008
Accepted October 16, 2008

IE801229Y